Research Square

Preprints are preliminary reports that have not undergone peer review.
They should not be considered conclusive, used to inform clinical practice,
or referenced by the media as validated information.

Revisiting Class IIb Histone Deacetylase Selectivity: Mechanistic Pitfalls and a Critical Bioactivity Audit of Reported HDAC1/HDAC6/HDAC10 Profiles

Evgenii Borisenko

evgeniabor11@gmail.com

- Laboratory of Molecular Neuroscience, Institute of Physical and Organic Chemistry, Southern Federal University, Rostov-on-Don, Russia https://orcid.org/0009-0007-3818-5118

Makar Andreev

ITMO University https://orcid.org/0009-0004-4908-2614

Research Article

Keywords: HDAC6, HDAC10, isoform selectivity, ChEMBL, difluoromethyloxadiazole, polyamine deacetylase, bioactivity data curation, machine learning in drug discovery

Posted Date: November 25th, 2026

DOI: https://doi.org/10.21203/rs.3.rs-11860185/v1

License: This work is licensed under a Creative Commons Attribution 4.0 International License.
Read Full License

Additional Declarations: The authors declare no competing interests.

Revisiting Class IIb Histone Deacetylase Selectivity: Mechanistic Pitfalls and a Critical Bioactivity Audit of Reported HDAC1/HDAC6/HDAC10 Profiles

Evgenii A. Borisenko[1,], Makar A. Andreev[2]*

1 - Laboratory of Molecular Neuroscience, Institute of Physical and Organic Chemistry, Southern Federal University, Rostov-on-Don, Russia

2 - Advanced Engineering School, ITMO University, St. Petersburg, Russia

** Corresponding author. Email: ebori@sfedu.ru*

Abstract. Selective targeting of histone deacetylase 6 (HDAC6) over Class I isoforms (notably HDAC1) has long served as a benchmark for avoiding epigenetic toxicity. However, discrimination against the fellow Class IIb member, HDAC10, represents an underappreciated pharmacological challenge. Here, we present a critical Perspective and bioactivity audit examining the concordance of HDAC1- and HDAC10-referenced selectivity across 466 small-molecule profiles (1,478 activity records from 162 source documents, 2007–2025) deposited in ChEMBL 37. In the primary unflagged exact-value cohort (347 profiles, 123 documents), HDAC1- and HDAC10-referenced selectivity margins show a high rank correlation (Spearman $\rho = 0.890$, 95% bootstrap CI 0.830–0.932). Among 149 profiles exhibiting ≥ 10-fold selectivity over HDAC1, 143 (96.0%) also satisfy a 10-fold margin over HDAC10. At a 100-fold threshold on both axes, 53 of 61 profiles (86.9%) remain concordant, while all 61 (100%) maintain at least 10-fold discrimination against HDAC10. A metadata audit, interpreted alongside verified biophysical profiles of benchmark inhibitors, indicates that this empirical database concordance is plausibly shaped in substantial part by historical assay formats: only 2 of 347 profiles explicitly employed an authentic polyamine substrate for HDAC10, whereas the remainder relied on generic acetyllysine peptides that HDAC10 poorly hydrolyzes. Furthermore, standard filtering for uncensored values eliminates mechanism-based difluoromethyl-1,3,4-oxadiazoles (DFMOs), which possess >3,300-fold selectivity but carry right-censored off-target limits. We synthesize recent structural enzymology (2017–2026) and outline four actionable principles intended to mitigate database bias in computational design and medicinal chemistry programs, whose quantitative impact on predictive model performance warrants dedicated prospective benchmarking.

Keywords: *HDAC6; HDAC10; isoform selectivity; ChEMBL; difluoromethyloxadiazole; polyamine deacetylase; bioactivity data curation; machine learning in drug discovery.*

1. Introduction: The Class IIb Selectivity Dilemma

Histone deacetylase 6 (HDAC6) is a predominantly cytoplasmic Class IIb enzyme whose canonical substrates include α-tubulin, cortactin, and heat shock protein 90 (HSP90)[1,2]. Over the past two decades, pharmacological inhibition of HDAC6 has been pursued across oncology, inflammatory disorders, and neurodegenerative conditions including amyotrophic lateral sclerosis (ALS) and ischemic stroke[3,4]. In experimental cerebral ischemia, HDAC6 is selectively upregulated in the cortical penumbra, and its targeted inhibition preserves acetylated α-tubulin, limits neuronal apoptosis, and accelerates functional recovery[5,6].

Historically, medicinal chemistry programs targeting HDAC6 have relied on counter-screening against Class I isoforms, particularly HDAC1, to avoid the hematological toxicity, gastrointestinal side effects, and cell-cycle arrest associated with pan-HDAC inhibition[3,7]. Reference probes such as Tubastatin A[3] and Nexturastat A[4] established the view that a bulky capping group or rigidified linker confers high (>100- to >1,000-fold) selectivity over HDAC1.

Selectivity, however, is defined only relative to a specified comparator under specified assay conditions. Strong discrimination against Class I enzymes does not guarantee selectivity over HDAC10, the other Class IIb isoform[7,8]. Despite sharing sequence homology and cytoplasmic localization, HDAC6 and HDAC10 govern distinct cellular processes. Whereas HDAC6 regulates microtubule stability and chaperone-dependent proteostasis, HDAC10 controls polyamine deacetylation and autophagic flux[7,9]. Unintended inhibition of HDAC10 perturbs spermidine metabolism and lysosomal homeostasis, complicating functional studies that attribute cellular phenotypes solely to HDAC6 blockade[8,9].

Public repositories such as ChEMBL assemble thousands of multi-target bioactivity records that now serve as default training sets for machine learning (ML) and quantitative structure–activity relationship (QSAR) models[10,11]. In many computational workflows, cataloged IC_{50} entries are pooled as uniform biophysical measurements. Here, we test that assumption by auditing reported HDAC1/HDAC6/HDAC10 activity profiles in ChEMBL 37 against the structural and mechanistic enzymology of Class IIb deacetylases.

2. Mechanistic and Structural Divergence of HDAC6 and HDAC10

The mechanistic understanding of Class IIb selectivity changed in 2017 when Christianson and co-workers solved the crystal structure of HDAC10 and established that it functions primarily as

a polyamine deacetylase (PDAC) rather than a protein lysine deacetylase[7]. HDAC10 displays high catalytic efficiency toward N^8-acetylspermidine, exceeding its activity on acetyllysine peptides by two orders of magnitude in k_{cat}/K_m[7]. This substrate preference is enforced by a constricted active-site channel and a negatively charged gatekeeper residue, Glu274 (human numbering; Glu272 in *Danio rerio*), which forms electrostatic and hydrogen-bonding interactions with the secondary ammonium group of polyamine substrates[7,8].

By contrast, HDAC6 contains tandem catalytic domains (CD1 and CD2)[1,2]. Its primary tubulin-deacetylating domain, CD2, features a wider and more adaptable catalytic entrance that accommodates bulky aromatic capping groups and surface-exposed acetyllysine residues without requiring an acidic gatekeeper contact[2,8].

This active-site divergence accounts for a major discrepancy in inhibitor profiling. Géraldy et al.[8] and Ptáček et al.[9] showed that classical "HDAC6-selective" hydroxamates, including Tubastatin A and Nexturastat A, inhibit or bind HDAC10 at low nanomolar concentrations (IC_{50} ≈ 4–24 nM)[8,9]. In Tubastatin A, the basic tertiary nitrogen within the tetrahydro-γ-carboline cap engages the Glu274 carboxylate of HDAC10, mimicking the positively charged polyamine tail[8]. Consequently, several benchmark hydroxamate probes behave as dual HDAC6/HDAC10 inhibitors when evaluated under substrate-appropriate biochemical or target-engagement conditions[9] (Table 1).

Table 1. *Benchmark HDAC6 inhibitors: Discrepancy between ChEMBL records and authentic biophysical profiling.*

Compound	ChEMBL ID	Reported ChEMBL 37 IC_{50} (nM)	Reported Margins	Verified Biophysical Profile[8,9]
Tubastatin A	CHEMBL2018302	HDAC6: 3.98 HDAC1: 1,412.5 HDAC10: 3,715.4	$S_{6/1}$ = 2.55 (355×) $S_{6/10}$ = 2.97 (933×)	Potent dual HDAC6/10 inhibitor (HDAC6 IC_{50} ≈ 4–15 nM; HDAC10 IC_{50} ≈ 4–24 nM vs. >30,000 nM in early peptide assays[3]). Binds Glu274 via basic cap amine[8,9].
Nexturastat A	CHEMBL2179618	HDAC6: 5.01 HDAC1: 3,020.0 HDAC10: 7,585.8	$S_{6/1}$ = 2.78 (602×) $S_{6/10}$ = 3.18 (1,514×)	Co-inhibits HDAC10 (HDAC6 IC_{50} = 3.8 nM; HDAC10 IC_{50} = 11 nM; actual

				selectivity margin 2.9-fold)[9].
Vorinostat (SAHA)	CHEMBL98	HDAC6: 14.13 HDAC1: 95.5 HDAC10: 72.4	$S_{6/1}$ = 0.83 (6.8×) $S_{6/10}$ = 0.71 (5.1×)	Broad-spectrum pan-HDAC inhibitor with modest discrimination across Class I and Class IIb.
Representative DFMO	CHEMBL5429808	HDAC6: 5.2 HDAC1: >100,000 HDAC10: >100,000	$S_{6/1}$ > 4.28 (>19,000×) $S_{6/10}$ > 4.28 (>19,000×)	Complete sparing of HDAC1 and HDAC10 in enzymatic and cellular assays. Excluded by exact-only database filters[9,12,13].

3. Chemical Evolution: From Hydroxamates to Mechanism-Based DFMOs

Recent medicinal chemistry efforts (2022–2026) have increasingly shifted away from unselective hydroxamic acid zinc-binding groups (ZBGs) toward chemotypes that exploit specific catalytic or structural features of individual Class IIb enzymes. The most consequential advance for selective HDAC6 targeting has been the characterization of difluoromethyl-1,3,4-oxadiazoles (DFMOs). As demonstrated by Cellupica et al.[12] and König et al.[13], DFMOs act as slow-binding, mechanism-based substrate analogs that undergo zinc-assisted hydrolytic ring opening selectively within the HDAC6 CD2 active site. Because the constricted HDAC10 site cannot efficiently catalyze this ring-opening reaction, DFMOs achieve long target residence times and >1,000- to >10,000-fold selectivity over both HDAC1 and HDAC10 in biochemical and cellular settings [9,12,13].

In parallel, non-hydroxamate hydrazide**s** have emerged as metabolically stable alternatives; Yue et al.[14] developed hydrazide 9m (HDAC6 IC_{50} = 21 nM), achieving >335-fold selectivity across tested HDAC isoforms and efficacy in NLRP3 inflammasome models. Within the central nervous system (CNS), James et al.[15] characterized EKZ-438, a brain-penetrant HDAC6 inhibitor that restores axonal transport in ALS and frontotemporal dementia models with verified in vivo target engagement. Hydroxamate optimization has also continued through linker rigidification, exemplified by the thiazole-linked *N*-hydroxypropanamides of Nam et al.[16] (~ 500-fold selectivity over HDAC1) and the neuroprotective tetrahydro-β-carboline derivatives of Wen et al.[20] (149-fold over HDAC1). Conversely, when selective HDAC10 inhibition is

desired, Steimbach et al.[17] showed that inserting a basic nitrogen atom at a defined position within the aliphatic linker of aza-SAHA probes (such as DKFZ-748) establishes a direct salt bridge with Glu274, reversing isoform preference toward HDAC10 (>60-fold over HDAC6).

4. Empirical Concordance in ChEMBL 37: Facts and Thresholds

To determine how Class IIb selectivity is represented across published bioactivity datasets, we audited a preselected ChEMBL 37 extraction comprising 466 compounds with same-document IC_{50} records for HDAC1, HDAC6, and HDAC10 across 162 source documents dated 2007–2025[10]. Selectivity margins were calculated from molar concentrations as:

$$S_{6/1} = \mathrm{pIC_{50}(HDAC6)} - \mathrm{pIC_{50}(HDAC1)} = \log_{10}\left[\frac{\mathrm{IC_{50}(HDAC1)}}{\mathrm{IC_{50}(HDAC6)}}\right]$$

$$S_{6/10} = \mathrm{pIC_{50}(HDAC6)} - \mathrm{pIC_{50}(HDAC10)} = \log_{10}\left[\frac{\mathrm{IC_{50}(HDAC10)}}{\mathrm{IC_{50}(HDAC6)}}\right]$$

Excluding 118 profiles with right-censored inequality bounds and one record carrying an unresolved tubacin/tubastatin A identity conflict yielded a primary exact-value cohort of 347 profiles from 123 documents, spanning 208 distinct Bemis–Murcko scaffolds (Section S1; Supplementary Dataset S1).

Across these 347 exact profiles, reported $S_{6/1}$ and $S_{6/10}$ margins correlate strongly (Spearman ρ = 0.890; 5,000-replicate document-cluster bootstrap 95% CI, 0.830–0.932; Figure 1). Leave-one-document-out sensitivity checks confirm that no single publication drives this relationship (ρ = 0.885–0.909). The association remains stable across stratified sub-cohorts: within hydroxamates alone (n = 273, 107 documents; ρ = 0.890, 10× retention 132/138 = 95.7%), among potent compounds with HDAC6 $IC_{50} \leq 1$ μM (n = 314; ρ = 0.890, 96.0%), and in studies published from 2017 onward (n = 154, 74 documents; ρ = 0.862, 73/76 = 96.1%; Table S1), although mixed-effects modeling across smaller non-hydroxamate scaffold clusters warrants future evaluation.

Threshold concordance depends directly on the chosen selectivity cutoff (Figure 2). When recalculated from unrounded nanomolar IC_{50} records, 149 profiles exhibit at least 10-fold preference for HDAC6 over HDAC1 ($S_{6/1} \geq 1.0$), and 143 of these (95.97% ≈ 96.0%; 95% bootstrap CI, 92.0–99.3%) also achieve a 10-fold margin over HDAC10. Using 2-decimal rounded pChEMBL values places two borderline compounds at $S_{6/1}$ = 1.00 (giving 145/151, or

96.03%), without altering the retention rate (Section S1.2; Table S1). At a 100-fold threshold on both axes ($S \geq 2.0$), concordance decreases to 53 of 61 profiles (86.89% ≈ 86.9%; 95% bootstrap CI, 76.8–94.7%). However, all 61 compounds with ≥ 100-fold selectivity over HDAC1 (100.0%; 95% CI, 94.1–100%) retain at least a 10-fold margin over HDAC10; the 8 discordant profiles maintain intermediate 26- to 66-fold discrimination ($S_{6/10}$ = 1.41–1.82; Table S3).

Because both $S_{6/1}$ and $S_{6/10}$ subtract an off-target value from the same pIC_{50}(HDAC6) term, arithmetic coupling contributes to their shared variance. Nevertheless, the underlying off-target potencies pIC_{50}(HDAC1) and pIC_{50}(HDAC10) correlate independently at $\rho = 0.874$ (95% CI 0.799–0.921; Figure S1), and the partial rank correlation between $S_{6/1}$ and $S_{6/10}$ conditioned on pIC_{50}(HDAC6) remains $\rho_{partial} = 0.875$. The database concordance therefore reflects genuine co-variation in reported off-target measurements rather than a purely mathematical identity.

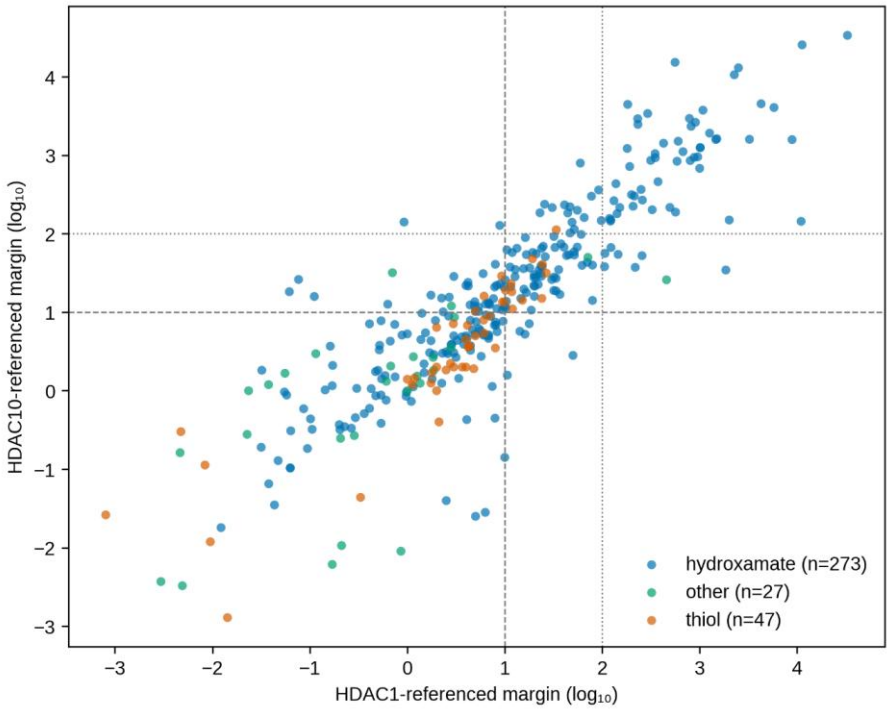

Figure 1. *Concordance of reported HDAC1- and HDAC10-referenced HDAC6 selectivity margins. Scatter plot of $S_{6/1}$ versus $S_{6/10}$ across 347 unflagged exact-value profiles from ChEMBL 37 (123 documents). Points are colored by structural zinc-binding motif: hydroxamates (blue, n = 273), thiols (orange, n = 47), and other chemotypes (green, n = 27). Dashed and dotted lines denote 10-fold and 100-fold selectivity thresholds, respectively. Spearman ρ = 0.890 (95% document-cluster bootstrap CI, 0.830–0.932).*

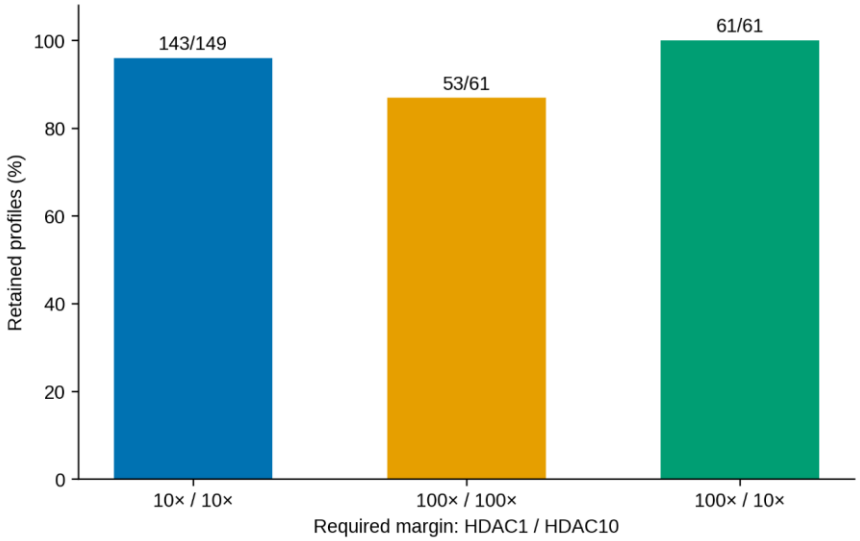

Figure 2. *Retention of HDAC10 discrimination across selectivity thresholds. Fractions of profiles retaining specified HDAC10 margins among compounds meeting HDAC1 criteria. Blue bar: 10× / 10× concordance (143/149; 96.0%). Orange bar: 100× / 100× concordance (53/61; 86.9%). Green bar: 100× HDAC1 / 10× HDAC10 retention (61/61; 100.0%). All compounds with ≥ 100-fold selectivity over HDAC1 retain at least 10-fold preference over HDAC10.*

5. Sources of Database Bias: Substrate Choice, Censoring, and Assay Mixing

To understand why aggregated ChEMBL profiles display 96% concordance whereas side-by-side biophysical studies reveal frequent HDAC10 cross-inhibition by HDAC6 probes[8,9], we inspected the 1,478 underlying activity records and assay descriptions. Three methodological factors explain this divergence.

5.1. The Substrate Blind Spot

Among the 347 exact profiles in the primary dataset, only 2 profiles explicitly documented a polyamine substrate (N^8-acetylspermidine or a fluorescent polyamine derivative) in their ChEMBL assay metadata. The remaining 345 profiles relied on generic acetyllysine peptide substrates originally optimized for Class I and Class IIa HDACs.

Because recombinant human HDAC10 shows minimal catalytic turnover on acetyllysine peptides[7], apparent IC_{50} values derived from peptidic assays may reflect low-efficiency residual cleavage or assay background rather than inhibition of physiological polyamine deacetylation[8,9].

For basic hydroxamates such as Tubastatin A and Nexturastat A, historical peptide-based entries in ChEMBL overestimate HDAC6/HDAC10 selectivity by two to three orders of magnitude compared with polyamine-substrate or target-engagement assays[8,9] (Table 1). This conclusion draws on polyamine-substrate measurements currently available for a limited set of reference hydroxamates and DFMOs[8,9,19]; because we did not perform experimental assays in-house, orthogonal re-profiling of a broader, chemotype-stratified compound panel using N^8-acetylspermidine reporters and cellular target engagement is needed to establish how widely this discrepancy extends across other scaffolds.

5.2. The Exact-Value Trap: Censoring Excludes Superior Chemotypes

A routine pre-processing step in QSAR and ML studies is restricting datasets to exact numeric IC_{50} records while discarding entries bearing inequality qualifiers (<, >, or ~)[11,18]. In the 466-compound export, 118 profiles (25.3%) contained at least one right-censored measurement.

As a consequence, all three DFMO derivatives in the cohort (CHEMBL5410192, CHEMBL5425061, and CHEMBL5429808, reported in 2024) were excluded from the exact-value subset. Each of these compounds inhibits HDAC6 at nanomolar concentrations (pIC_{50} = 7.52–8.29; IC_{50} = 5.2–30 nM) while showing no measurable inhibition of HDAC1 or HDAC10 up to 100 μM (recorded as IC_{50} > 100,000 nM, $pIC_{50} \leq 4.0$), corresponding to selectivity margins above 3,300- to 19,000-fold (Table S2B). When all 118 censored profiles are analyzed via conservative interval bounds rather than omitted, 52 profiles (including all three DFMOs) are confirmed to meet or exceed the 10-fold selectivity threshold, 16 fall below the threshold, and 50 remain unresolved due to dual off-target right-censoring (Table S2A); a complete censored-aware rank recalculation on polyamine-verified datasets is warranted to quantify the resulting shift in global correlation. Removing right-censored records therefore systematically strips training sets of the most selective inhibitor classes.

5.3. Assay Mixing Within Source Documents

Selecting measurements from the same publication reduces inter-laboratory variance but does not guarantee uniform assay formats[18]. Within the 347 exact profiles, 22 pooled multiple assay identifiers for at least one target.

Among the 6 tenfold discordant profiles ($S_{6/1} \geq 1.0$ but $S_{6/10} < 1.0$; Table 2), two compounds (CHEMBL2018451 and CHEMBL4470067, both from document CHEMBL4385610) combined

an enzymatic deacetylation assay for HDAC1 with an intracellular NanoBRET displacement assay for HDAC6 and a TR-FRET tracer binding assay for HDAC10. Ratios constructed across enzymatic and binding readouts cannot be interpreted as equivalent catalytic selectivity factors.

5.4. Physicochemical Trends

Exploratory comparison of RDKit descriptors indicates that profiles retaining a ≥ 10-fold margin over both comparators have lower median molecular weight (391.9 vs 420.5 g/mol; Benjamini–Hochberg adjusted q = 0.0078; Figure S2a) and fewer rotatable bonds (median RotB = 7 vs 9; q = 0.00013) than profiles below the threshold. Within the hydroxamate subset (N = 273), the difference in rotatable bonds remains statistically significant (q = 0.00099), whereas molecular weight softens (q = 0.0588; Table S4). Because related analogs cluster within individual publications (for example, 32 of 47 thiol profiles originate from a single source document), these descriptor shifts represent descriptive corpus trends rather than causal design rules.

Table 2. *Assay and potency breakdown of the six 10-fold discordant profiles ($S_{6/1} \geq 1.0$ but $S_{6/10} < 1.0$).*

Molecule ID	Document ID	HDAC6 (nM)	HDAC1 (nM)	HDAC10 (nM)	$S_{6/1}$	$S_{6/10}$	Assay Context and Interpretation
CHEMBL2018451	CHEMBL4385610	63.1	3,162.3	177.8	1.70	0.45	Mixed endpoints: HDAC1 (deacetylation), HDAC6 (cellular BRET), HDAC10 (TR-FRET tracer binding).
CHEMBL4470067	CHEMBL4385610	125.9	1,258.9	17.8	1.00	-0.85	Mixed endpoints from the same study; higher affinity for HDAC10 in TR-FRET binding.
CHEMBL2414098	CHEMBL2413017	1.91	19.95	3.02	1.02	0.20	Potent nanomolar inhibitor across all three enzymes; lies directly on the 10-fold HDAC1 boundary.
CHEMBL3426803	CHEMBL3425488	7.08	100.0	39.8	1.15	0.75	Homogeneous fluorescence release assay; retains 5.6-fold preference over HDAC10.
CHEMBL5271192	CHEMBL5252522	79.4	1,288.3	416.9	1.21	0.72	Hydroxamate bearing a basic amine motif; 16-fold over HDAC1

							vs. 5.2-fold over HDAC10.
CHEMBL5594027	CHEMBL5579854	46.8	831.8	331.1	1.25	0.85	Recombinant baculovirus-expressed enzyme panel; retains 7.1-fold selectivity over HDAC10.

6. Perspective and Actionable Guidelines for Drug Discovery

The finding that HDAC1- and HDAC10-referenced margins correlate at $\rho = 0.890$ in ChEMBL 37 summarizes historical literature practices dominated by acetyllysine peptide assays, rather than certified enzymatic selectivity. Because we have not trained QSAR or machine learning models here, the quantitative impact of censored-aware and substrate-aware curation on predictive accuracy requires dedicated prospective benchmarking. Nevertheless, integrating recent Class IIb structural enzymology with our database audit supports four practical recommendations:

1. Substrate-Appropriate Isoform Profiling: Counter-screening against Class I HDACs (HDAC1/2/3) cannot substitute for direct HDAC10 testing. Enzymatic HDAC10 assays should employ validated polyamine substrates such as N^8-acetylspermidine or fluorescent polyamine reporters[19], complemented by intracellular target-engagement readouts (NanoBRET or CETSA).

2. Censored-Aware Machine Learning: Computational workflows should retain right-censored off-target records (IC_{50} > limit) as informative lower bounds on selectivity. Interval-censored regression, Tobit models, or survival-based objectives are expected to prevent the systematic loss of high-selectivity chemotypes such as DFMOs and should be directly benchmarked on HDAC datasets.

3. Caution with Basic Capping Groups: In HDAC6 lead optimization, introducing basic secondary or tertiary amines into the cap or linker increases the likelihood of electrostatic engagement with the Glu274 gatekeeper of HDAC10. Such motifs require early counter-screening in a polyamine-based HDAC10 assay.

4. Mechanism-Based Selectivity for Biological Probes: When experimental hypotheses require strict isolation of HDAC6 catalytic activity, such as evaluating microtubule stabilization and

neuroprotection in stroke or ALS models[5,6,15], mechanism-based inhibitors (DFMOs) provide cleaner pharmacological separation from HDAC10 than classical reversible hydroxamates.

Contributions. Evgenii Borisenko – Conceptualization, Data curation, Writing original draft; Makar Andreev – Formal analysis (bibliometric data), Data curation, Writing original draft.

Funding. This study was supported by Ministry of Science and Education FENW, 2026-0009.

Compliance with ethical standards. This article does not contain any studies with human participants performed by any of the authors.

Conflict of interest. The authors declare that they have no conflicts of interest.

Data Availability Statement. The audited ChEMBL 37 dataset supporting the findings of this study is provided in the Supporting Information. All bioactivity records were retrieved from the publicly available ChEMBL 37 database (*https://www.ebi.ac.uk/chembl/*).

References

1. Hubbert, C. et al. HDAC6 is a microtubule-associated deacetylase. Nature 417, 455-8 (2002). https://doi.org/10.1038/417455a PMID: 12024216.

2. Haggarty, S.J. et al. Domain-selective small-molecule inhibitor of histone deacetylase 6 (HDAC6)-mediated tubulin deacetylation. Proc Natl Acad Sci U S A 100, 4389-94 (2003). https://doi.org/10.1073/pnas.0430973100 PMID: 12677000.

3. Butler, K.V. et al. Rational design and simple chemistry yield a superior, neuroprotective HDAC6 inhibitor, tubastatin A. J Am Chem Soc 132, 10842-6 (2010). https://doi.org/10.1021/ja102758v PMID: 20614936.

4. Bergman, J.A. et al. Selective histone deacetylase 6 inhibitors bearing substituted urea linkers inhibit melanoma cell growth. J Med Chem 55, 9891-9 (2012). https://doi.org/10.1021/jm301098e PMID: 23009203.

5. Demyanenko, S.V., Dzreyan, V.A. & Uzdensky, A.B. Overexpression of HDAC6, but not HDAC3 and HDAC4 in the penumbra after photothrombotic stroke in the rat cerebral cortex and the neuroprotective effects of α-phenyl tropolone, HPOB, and sodium valproate. Brain Res Bull 162, 151-165 (2020). https://doi.org/10.1016/j.brainresbull.2020.06.010 PMID: 32592806.

6. Demyanenko, S., Dzreyan, V. & Sharifulina, S. Histone Deacetylases and Their Isoform-Specific Inhibitors in Ischemic Stroke. Biomedicines 9, 1445 (2021). https://doi.org/10.3390/biomedicines9101445 PMID: 34680562.

7. Hai, Y. et al. Histone deacetylase 10 structure and molecular function as a polyamine deacetylase. Nat Commun 8, 15368 (2017). https://doi.org/10.1038/ncomms15368 PMID: 28516954.

8. Géraldy, M. et al. Selective Inhibition of Histone Deacetylase 10: Hydrogen Bonding to the Gatekeeper Residue is Implicated. J Med Chem 62, 4426-4443 (2019). https://doi.org/10.1021/acs.jmedchem.8b01936 PMID: 30964290.

9. Ptacek, J. et al. Selectivity of Hydroxamate- and Difluoromethyloxadiazole-Based Inhibitors of Histone Deacetylase 6 In Vitro and in Cells. Int J Mol Sci 24, 4720 (2023). https://doi.org/10.3390/ijms24054720 PMID: 36902164.

10. Zdrazil, B. et al. The ChEMBL Database in 2023: a drug discovery platform spanning multiple bioactivity data types and time periods. Nucleic Acids Res 52, D1180-D1192 (2024). https://doi.org/10.1093/nar/gkad1004 PMID: 37933841.

11. Landrum, G.A. & Riniker, S. Combining IC50 or Ki Values from Different Sources Is a Source of Significant Noise. J Chem Inf Model 64, 1560-1567 (2024). https://doi.org/10.1021/acs.jcim.4c00049 PMID: 38394344.

12. Cellupica, E. et al. Difluoromethyl-1,3,4-oxadiazoles are slow-binding substrate analog inhibitors of histone deacetylase 6 with unprecedented isotype selectivity. J Biol Chem 299, 102800 (2023). https://doi.org/10.1016/j.jbc.2022.102800 PMID: 36528061.

13. König, B. et al. Difluoromethyl-1,3,4-oxadiazoles Are Selective, Mechanism-Based, and Essentially Irreversible Inhibitors of Histone Deacetylase 6. J Med Chem 66, 13821-13837 (2023). https://doi.org/10.1021/acs.jmedchem.3c01345 PMID: 37782298.

14. Yue, K. et al. Development of Hydrazide-Based HDAC6 Selective Inhibitors for Treating NLRP3 Inflammasome-Related Diseases. J Med Chem 68, 9279-9302 (2025). https://doi.org/10.1021/acs.jmedchem.4c02883 PMID: 40193276.

15. James, R.E. et al. A next-generation HDAC6 inhibitor for amyotrophic lateral sclerosis and frontotemporal dementia. Brain 149, 1586-1603 (2026). https://doi.org/10.1093/brain/awaf380 PMID: 41061670.

16. Nam, G. et al. Thiazole-Linked N-Hydroxypropanamide Derivatives: Selective HDAC6 Inhibitors with Therapeutic Potential for Neurodegenerative Diseases. J Med Chem 69, 14140-14155 (2026). https://doi.org/10.1021/acs.jmedchem.5c03292 PMID: 42241502.

17. Steimbach, R.R. et al. Aza-SAHA Derivatives Are Selective Histone Deacetylase 10 Chemical Probes That Inhibit Polyamine Deacetylation and Phenocopy HDAC10 Knockout. J Am Chem Soc 144, 18861-18875 (2022). https://doi.org/10.1021/jacs.2c05030 PMID: 36200994.

18. Kalliokoski, T. et al. Comparability of mixed IC_{50} data - a statistical analysis. PLoS One 8, e61007 (2013). https://doi.org/10.1371/journal.pone.0061007 PMID: 23613770.

19. Herp, D. et al. First Fluorescent Acetylspermidine Deacetylation Assay for HDAC10 Identifies Selective Inhibitors with Cellular Target Engagement. Chembiochem 23, e202200180 (2022). https://doi.org/10.1002/cbic.202200180 PMID: 35608330.

20. Wen, W. et al. Re-exploration of tetrahydro-β-carboline scaffold: Discovery of selective histone deacetylase 6 inhibitors with neurite outgrowth-promoting and neuroprotective activities. Bioorg Med Chem Lett 102, 129670 (2024). https://doi.org/10.1016/j.bmcl.2024.129670 PMID: 38387692.

Supplementary Files

This is a list of supplementary files associated with this preprint. Click to download.

- SupplementaryDatasetS1.xlsx
- SupportingInformation.docx